EFFECTS OF ALLOYING ELEMENTS ON ELASTIC PROPERTIES OF Al BY FIRST-PRINCIPLES CALCULATIONS

J. Wang [a, b, c, *], Y. Du [b], S.-L. Shang [c], Z.-K. Liu [c], Y.-W. Li [b]

[a] School of Metallurgy and Environment, Central South University, Changsha, Hunan, China
[b] State Key Laboratory of Powder Metallurgy, Central South University, Changsha, Hunan, China
[c] Department of Materials Science and Engineering, The Pennsylvania State University, University Park, Pennsylvania, USA

Abstract

The effects of alloying elements (Co, Cu, Fe, Ge, Hf, Mg, Mn, Ni, Si, Sr, Ti, V, Y, Zn, and Zr) on elastic properties of Al have been investigated using first-principles calculations within the generalized gradient approximation. A supercell consisting of 31 Al atoms and one solute atom is used. A good agreement is obtained between calculated and available experimental data. Lattice parameters of the studied Al alloys are found to be depended on atomic radii of solute atoms. The elastic properties of polycrystalline aggregates including bulk modulus (B), shear modulus (G), Young's modulus (E), and the B/G ratio are also determined based on the calculated elastic constants (c_{ij}'s). It is found that the bulk modulus of Al alloys decreases with increasing volume due to the addition of alloying elements and the bulk modulus is also related to the total molar volume (V_m) and electron density ($n_{Al_{31}X}$) with the relationship of $n_{Al_{31}X} = 1.0594 + 0.0207\sqrt{B/V_m}$. These results are of relevance to tailor the properties of Al alloys.

Key words: Aluminum alloys; Elastic properties; First-principles calculations;

1. Introduction

With a density approximately one third of that of steel or copper, aluminum (Al) alloys with alloying elements Cu, Mg, Si, Zn, and Zr, etc, are widely used as engineering materials where light weight or corrosion resistance is required. The properties of Al, which make this metal and its alloys the most economical and attractive for a wide variety of uses, are appearance, light weight, fabric ability, physical properties, mechanical properties, and corrosion resistance [1-2]. Therefore, a detailed understanding of the thermodynamic and elastic properties of Al alloys is crucial for a better realization of its potential in currently available applications and in developing new ones. The thermodynamic modeling through integrating first-principles calculations and CALPHAD (CALculation of PHAse Diagram) method has proven to be efficient and robust [3] and demonstrated for relevant binary, ternary and multi-component systems of Al alloys of [4]. Recently, the enthalpies of formation and elastic properties for binary Al compounds were systematically predicted by first-principles calculations [5]. However, there are no theoretical studies addressing the elastic property

changes in Al induced by alloying elements.

It is known that the elastic properties of materials can be used to assess certain mechanical properties such as ductility/brittleness, hardness, strength and so on [6]. The theoretical prediction for the effect of alloying additions on the elastic constants (c_{ij}'s) can provide essential guidance in identifying materials with desired mechanical properties[7]. The effects of alloying elements on the elastic properties of AlTi and AlTi$_3$ [8], AlNi [9], AlNi$_3$ [10], Mg [11] and Ni [12] were studied via first-principles approach. These works are important for tailoring the properties of existed alloys and designing new alloys. In this paper, the effects of alloying elements (Co, Cu, Fe, Ge, Hf, Mg, Mn, Ni, Si, Sr, Ti, V, Y, Zn, and Zr) on the elastic properties in the Al dilute solid solutions are predicted via first-principles calculations using the efficient stress-strain method [13]. The present work, together with the previous work [5] on the elastic constants of compounds, forms a basis for predicting the elastic properties of Al alloys. It is our ambition to spark systematic experimental studies of the elastic properties with this contribution.

The rest of the present paper is described as follows: the details of first-principles calculations

using Vienna Ab-inito Simulation Package (VASP) [14-15] are presented in Section 2, including the brief introduction of equation of state (EOS) and elastic theory used herein. In Section 3, The investigated equilibrium properties include the volume (V_0), energy (E_0), bulk modulus (B_0) and its pressure derivative (B_0') of the compounds, determined via EOS fitting, and the single crystal elastic constants (c_{ij}'s) together with structural stabilities and the polycrystalline aggregates are presented and discussed. Finally in Section 4, the summary of the present work is given.

2. Theory and methodology

First-principles calculations are performed using the VASP [14-15] code with the projected augment wave (PAW) [16-17] method to describe the electron-ion interaction and the generalized gradient approximation (GGA) [18] to depict the exchange-correction functional. All the structures are fully relaxed with respect to cell shape, volume, and atomic coordinates. For consistency, a 400 eV energy cutoff is used for all the elements. A $2\times2\times2$ fcc (face-centered-cubic) supercell including 31 Al atoms and one alloying atom (X) is employed in this study. The energy convergence criterion of electronic self-consistency is chosen as 10^{-6} eV/atom for all the calculations. The reciprocal space energy integration is performed by the Methfessel-Paxton technique [19] for structure relaxations, while the final calculations of total energies for EOS fittings and stresses for determining the c_{ij}'s are performed by the linear tetrahedron method including Blöchl corrections [20]. The samplings of k-point are $15\times15\times15$ and $11\times11\times11$ for EOS and elastic constants calculations in terms of the Monkhorst-Pack [21] scheme, respectively.

In order to fit the first-principles calculated E-V (energy-volume) data points, the 4-parameter Birch-Murnaghan equation of state with its linear form given by Shang et al. [22] is employed,

$$E(V) = a + bV^{-2/3} + cV^{-4/3} + dV^{-2} \tag{1}$$

where a, b, c and d are fitting parameters. In the present work, usually 10 data points in the volume range of 0.88-$1.16V_0$ are used for the EOS fitting of each structure. The equilibrium properties estimated from EOS include the volume (V_0), energy (E_0), bulk modulus (B_0) and its pressure derivative (B_0'). It is worth mentioning that the fitting parameters are representable by the equilibrium properties, and *vice versa* [22].

In an effort to calculate the single crystal elastic stiffness constants c_{ij}'s, an efficient strain-stress method proposed by Shang et al. [13] is employed in the present work. Under this methodology, for a given

set of strains $\epsilon = (\epsilon_1, \epsilon_2, \epsilon_3, \epsilon_4, \epsilon_5, \epsilon_6)$ (where ϵ_1, ϵ_2 and ϵ_3 are the normal strains and ϵ_4, ϵ_5 and ϵ_6 are the shear strains) imposed on a crystal with lattice vectors $\mathbf{L}$ specified in the Cartesian coordinates

$$L = \begin{pmatrix} a_1 & a_2 & a_3 \\ b_1 & b_2 & b_3 \\ c_1 & c_2 & c_3 \end{pmatrix} \tag{2}$$

where a_1, a_2 and a_3 are the x, y, z components of the lattice vector $\mathbf{a}$, respectively, and it is the same for lattice vectors $\mathbf{b}$ and $\mathbf{c}$. After the deformation due to strain ϵ, the deformed lattice vectors are obtained as follows:

$$L_{def} = L \begin{pmatrix} 1+\varepsilon_1 & \varepsilon_6/2 & \varepsilon_5/2 \\ \varepsilon_6/2 & 1+\varepsilon_2 & \varepsilon_4/2 \\ \varepsilon_5/2 & \varepsilon_4/2 & 1+\varepsilon_3 \end{pmatrix} \tag{3}$$

Accordingly, a set of stresses, $\boldsymbol{\sigma} = (\sigma_1, \sigma_2, \sigma_3, \sigma_4, \sigma_5, \sigma_6)$, associated with the deformed crystal will be determined through first-principles calculations in the present work. Correspondingly, for n sets of strains ϵ (n-by-6 matrix) and the resulting stresses $\boldsymbol{\sigma}$, the elastic constants c (6-by-6 matrix as shown in Voigt's notation.) are determined according to the general Hooke's law as follows:

$$\begin{pmatrix} c_{11} & c_{12} & c_{13} & c_{14} & c_{15} & c_{16} \\ c_{21} & c_{21} & c_{21} & c_{21} & c_{21} & c_{21} \\ c_{31} & c_{32} & c_{33} & c_{34} & c_{35} & c_{36} \\ c_{41} & c_{42} & c_{43} & c_{44} & c_{45} & c_{46} \\ c_{51} & c_{52} & c_{53} & c_{54} & c_{55} & c_{56} \\ c_{61} & c_{62} & c_{63} & c_{64} & c_{65} & c_{66} \end{pmatrix} = \begin{pmatrix} \varepsilon_{1,1} & \varepsilon_{1,n} \\ \varepsilon_{2,1} & \varepsilon_{2,n} \\ \varepsilon_{3,1} & \varepsilon_{3,n} \\ \varepsilon_{4,1} \cdots \varepsilon_{4,n} \\ \varepsilon_{5,1} & \varepsilon_{5,n} \\ \varepsilon_{6,1} & \varepsilon_{6,n} \end{pmatrix}^{-1} \begin{pmatrix} \sigma_{1,1} & \sigma_{1,n} \\ \sigma_{2,1} & \sigma_{2,n} \\ \sigma_{3,1} \cdots \sigma_{3,n} \\ \sigma_{4,1} & \sigma_{4,n} \\ \sigma_{5,1} & \sigma_{5,n} \\ \sigma_{6,1} & \sigma_{6,n} \end{pmatrix} \tag{4}$$

where "-1" represents the pseudo-inverse, which can be solved based on the singular value decomposition method to get the least square solutions of elastic constants. Due to the symmetry of crystals, the minimum linearly independent sets of strains to determine the elastic constants are two for cubic, three for hexagonal and rhombohedral, four for tetragonal, and six for orthorhombic, monoclinic, and triclinic structures [13, 23]. In this work, the following linearly independent sets of strains are selected:

$$\begin{pmatrix} x & 0 & 0 & 0 & 0 & 0 \\ 0 & x & 0 & 0 & 0 & 0 \\ 0 & 0 & x & 0 & 0 & 0 \\ 0 & 0 & 0 & x & 0 & 0 \\ 0 & 0 & 0 & 0 & x & 0 \\ 0 & 0 & 0 & 0 & 0 & x \end{pmatrix}$$
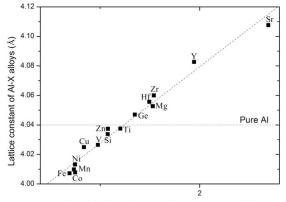
with $x=\pm0.007$, and ±0.01, which are verified to obey the Hooke's law, leading to a sufficient redundancy of the nonzero stresses and in turn accurate elastic constants.

Based on c_{ij}'s, polycrystalline aggregates, including the bulk (B), shear (G), and Young's (E)

modulus, can be computed via the Voigt's approach [24], viz, $B = (c_{11} + 2c_{12})/3$, $G = (c_{11} - c_{12} + 3c_{44})/5$ and $E = 9BG/(G + 3B)$ for cubic structures. More details regarding the calculations of elastic constants and the applications of strain-stress method can be found elsewhere [13, 25-27].

3. Results and discussion

Calculated lattice parameters of pure fcc Al and Al-X alloys along with the available experimental data are summarized in Table 1. Among the 15 Al-X alloys studied herein, experimental data are available for Al-Fe [28], Al-Si [29], and Al-Ti [30] from X-ray diffraction (XRD) as shown in Table 1. A good agreement is obtained between the calculated and experimental data, with the differences of -0.51%, -0.23%, and -0.16% for Al-Fe, Al-Si, and Al-Ti, respectively. It is found in Table 1 that the lattice parameters of Al-X alloys are proportional to the corresponding lattice parameter of pure element X in the fcc structure [31]. Figure 1 depicts the change of the lattice parameter of Al due to the addition of solute elements in comparison with the atomic radii of solute atoms calculated from their fcc structures. Here, the atomic radii of pure elements are calculated as half of the nearest-neighbor atomic distance, being consistent with those calculated by Wang et al. [31]. Figure 2 shows the change of the nearest-neighbor distance between Al and X atom against the atomic radii of

Figure 1. *Influence of atomic radius of solute atom (X) on lattice constant of Al-3.125 at. % X solution.*

solute atoms. The nearest-neighbor distance between Al and X show a similar relationship against atomic radii of solute atoms.

For dilute solutions the change of lattice parameter can be treated as a linear function of composition according to Wang et al. [32]. The linear regression coefficients for each element are calculated using the following equation [32]:

$$k_x = N(a_{Al_{31}X} - a_{Al_{32}})/100 \qquad \text{[pm/at. %]} \qquad (5)$$

where N is the number of atoms in the supercell (N = 32 for the present work), $a_{Al_{31}X}$ the lattice parameter

Table 1. *Lattice parameters of Al-3.125X (X in at. %) fcc dilute solutions and linear regression coefficients of Eq. 5.*

Alloying element (X)	Lattice parameters (Å)			Lattice parameter of pure element [a] (Å)	Nearest-neighbor distance between Al and X (Å)	Linear regression coefficient (pm/at. %)
	Calc.	Expt.	Diff. (%)			
Al	4.046	4.049 [b]	-0.07	4.048	2.861	-
Al (32 atoms)	4.04	4.049 [b]	-0.22	4.048	2.856	-
Co	4.008			3.518	2.748	-1.0365
Cu	4.025			3.631	2.808	-0.4887
Fe	4.007	4.0275 [c]	-0.51	3.446	2.738	-1.055
Ge	4.047			4.284	2.882	0.2158
Hf	4.056			4.471	2.888	0.4938
Mg	4.053			4.516	2.892	0.3997
Mn	4.01			3.502	2.737	-0.9714
Ni	4.013			3.517	2.772	-0.8631
Si	4.034	4.0435 [d]	-0.23	3.936	2.839	-0.2058
Sr	4.108			6	3.048	2.1576
Ti	4.038	4.0445 [e]	-0.16	4.099	2.828	-0.0861
V	4.026			3.81	2.79	-0.4391
Y	4.083			5.046	2.974	1.3592
Zn	4.037			3.939	2.849	-0.09
Zr	4.06			4.529	2.901	0.6325

[a] *lattice parameters in the fcc structure [31];* [b] *Pearson handbook [45];* [c] *Ref. [28];* [d] *Ref. [29];* [e] *Ref. [30].*
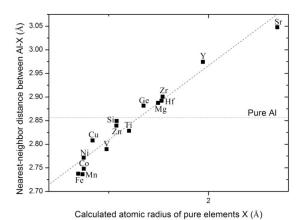
Figure 2. Correlation between atomic radius of solute atom (X) and the nearest-neighbor distance between Al and X in Al-3.125 at. % X solution.

of the cell with 31 Al atoms and one X atom, and $a_{Al_{32}}$ the lattice parameters of the cell with 32 Al atoms. The calculated linear regression coefficients are listed in Table 1. The linear regression coefficient of Ti and Zn are almost zero indicating that the lattice parameter rarely changes due to their additions, which also can be seen in Figure 1.

The changes of the nearest-neighbor distance around a solute atom can be described by local lattice distortion which is listed in Table 2 along with available experimental measurements [33]. The calculated local lattice distortions in the present work are within the experimental uncertainties for Cu, Ge, Mn, and Zn [33], as shown in Figure 3. The local lattice distortion due to the addition of Zn is the closest to experimental data. This also verifies the zero linear regression coefficient of Zn shown in Table 1.

The predicted properties for Al-3.125X (at.%) dilute solid solutions, including the elastic constants (c_{11}, c_{12} and c_{44}), the bulk modulus (B), shear modulus
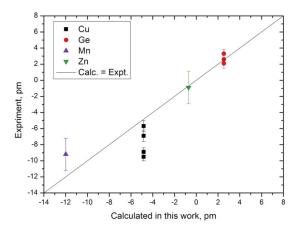

Figure 3. Calculated local lattice distortion compared with experimental data [33].

Table 2. *Local lattice distortions in fcc Al-X solutions in pm.*

Alloying element (X)	This work	Expt. [33]
Al	-	-
Co	-10.84	-
Cu	-4.84	-5.7±0.7
		-6.9±0.7
		-8.9±0.5
		-9.5±0.5
Fe	-11.87	-
Ge	2.53	2.1±0.6
		2.6±0.5
		3.3±0.5
Hf	3.12	-
Mg	3.58	-
Mn	-11.99	-9.2±2.0
Ni	-8.47	-
Si	-1.7	-
Sr	19.15	-
Ti	-2.81	-
V	-6.69	-
Y	11.81	-
Zn	-0.71	-0.9±2.0
Zr	4.44	-

(G), Young's (E) modulus, and B/G ratio along with the available experimental data are shown in Table 3. The estimated bulk modulus and equilibrium volume using EOS (Eq. 1) are also shown for comparison. The fitting error (Eq. 4 in Ref. [26]) of EOS is smaller than 0.1, indicates the high qualities of first-principles calculations. The bulk moduli of Al-X dilute solutions calculated using the two methods (c_{ij}'s and EOS) are very close to each other. The bulk moduli obtained from EOS are slightly smaller than those from c_{ij}'s, since the volume ranges used in EOS fitting are wider [13]. The available experimental data for Al-X dilute alloys are for Al-Cu [24, 34] and Al-Mg [35]. The reported c_{ij}'s for Al-5Cu (at. %) are 308.22, 262.56, and 27.03 GPa for c_{11}, c_{12}, and c_{44}, respectively, where c_{11} and c_{12} are much larger than the calculated values at Al-3.125Cu (at. %). The extremely large c_{11} and c_{12} thus result in unreasonable large bulk modulus (277.8) and B/G ratio (10.9). This is probably due to the samples were in precipitation hardened state and texture were existence. The calculated and experimental elastic properties data for the Al-3.125Mg (at. %) solid solution is compared in Figure 4. It should be mentioned that the experimental elastic constants of Al-Mg [35] alloy with composition of 3.125 at % Mg are obtained by linear interpolation. The calculated values are slightly larger than experimental data, which is reasonable since the first-principles calculations are performed at 0 K, while the experimental data were measured at room

temperature, and elastic constants decrease with increasing temperature [36]. All the alloy systems shown in Table 3 satisfy the Born criteria [37-38] for mechanical stability, i.e., $c_{11} - |c_{12}| > 0$, $c_{11} + 2|c_{12}| > 0$ and $c_{44} > 0$ for cubic structure, indicating that the Al alloys with 3.125%X are within the limit of mechanical stability.

Figure 5 shows that the calculated bulk moduli of Al-X alloys decrease linearly with respect to the increase of nearest-neighbor distances between Al and X atoms. The smallest bulk modulus is due to the addition of Sr, while the largest one is due to the addition of Fe among all the Al alloys studied in the present work. It can also be seen from Figure 6 which
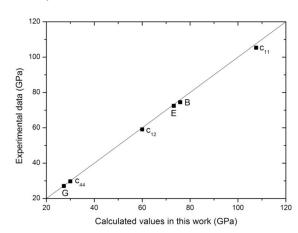

Figure 4. *Calculated elastic constants of Al-3.125 Mg at. % binary solid solution in the present work along with experimental data [35].*

Figure 5. *Correlation between bulk modulus and nearest-neighbor distance in Al-3.125 at. % X solution.*

Table 3. *Calculated properties of Al-3.125X (at. %) dilute solid solutions: equilibrium volume (V, Å³), elastic constants (c_{11}, c_{12} and c_{44}), bulk modulus (B), shear modulus (G), Young's (E) modulus, and B/G ratio along with available experimental data. The unit for elastic properties is GPa.*

Alloying element (X)	V_0	B_0	c_{11}	c_{12}	c_{44}	B	G	E	B/G
Al (expt.) [a]	16.595	~80	114.3	61.9	31.6	79.4	29.4	78.6	2.7
Al [b]	16.487	77.2	119.1	56.5	32.3	77.4	31.9	84.1	2.43
Co	16.094	82.9	110	69.7	36.2	83.1	28.6	77	2.9
Cu	16.301	79.3	115.9	62.6	33.5	80.4	30.8	81.3	2.61
Cu [c]	-	-	308.22	262.56	27.03	277.8	25.4	73.8	10.9
Fe	16.087	83.3	104.9	72.8	35.5	83.5	25.8	70.2	3.24
Ge	16.57	76.2	94	68.4	26.3	76.9	20.9	57.5	3.68
Hf	16.677	79.7	102.4	69.8	25.5	80.6	21.8	60	3.69
Mg	16.641	75.6	107.6	60	30	75.9	27.3	73.2	2.77
Mg [d]	-	-	105.3	59.1	29.7	74.5	27.1	72.5	2.75
Mn	16.119	83.3	121	65.2	40.2	83.8	34.7	91.6	2.41
Ni	16.159	81.7	130.3	58.2	34.2	82.2	34.9	91.8	2.35
Si	16.409	77.6	124	54.7	33.1	77.8	33.7	88.4	2.31
Sr	17.327	68.4	100.3	53.6	31.2	69.2	27.8	73.5	2.49
Ti	16.455	80.3	104.6	69.5	28.4	81.2	23.4	64.1	3.47
V	16.32	81.4	112.9	66.2	36.4	81.8	30.5	81.3	2.68
Y	17.013	74.5	98.4	63.7	30.8	75.3	24.4	66.1	3.08
Zn	16.453	77.1	112.4	60.3	29	77.7	27.8	74.5	2.8
Zr	16.731	79.2	100.2	69.8	21.1	79.9	18.7	52.1	4.27

[a] *Ref. [24];* [b] *32-atoms supercell;* [c] *Ref. [24, 34] for Al-5 at. % Cu (for reference only due to unreasonable large c_{11} and c_{12}). ;* [d] *Ref [35]*

shows a strong dependence of the bulk modulus on the atomic volume of the alloys, due to the addition of the alloying element. The calculated bulk moduli of Al-X alloys is further plotted in Figure 7 with respect to the bulk modulus of pure solute atom X. Alloying elements with higher bulk moduli, such as Co, Mn, Fe, and Mn result in the higher bulk moduli of Al-X alloys, and *vice versa*.
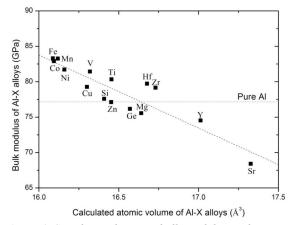

Figure 6. *Correlation between bulk modulus and atomic volume of Al-3.125 at.% X solution.*

According to Pugh criterion [39], a metal can be considered to be brittle when its bulk/shear modulus ratio is smaller than 1.75, otherwise ductile. All Al-X dilute solid solutions have their *B/G* ratios greater than 1.75, as shown in Table 3. This means Al will

remain be ductility with the addition of alloying element.

To understand which factors are correlated with the bulk modulus, Kim et al [10, 12] used the empirical relationship between the bulk modulus and volume reported by Miedema et al. [40]. According to Miedema et al. [40] and Li and Wu [41], $\sqrt{B/V_m}$ has a linear relationship with the change of electron density, n, at the boundary of Wigner-Seitz cell for pure elements, where V_m is the molar volume of the element for alkali metals and non-transition metals. The electron density n of $Al_{31}X$ solution can be calculated by the following equation [41]:

$$n_{Al_{31}X} = N_{Al_{31}X} / V_{Al_{31}X} = (\frac{31}{32} n_{Al} V_{Al} + \frac{1}{32} n_X V_X) \quad (6)$$
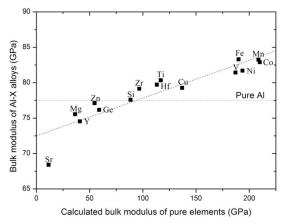

Figure 7. *Influence of bulk modulus of solute atom (X) on the bulk modulus of Al-3.125 at. % X solution.*

Table 4. *Volume (V), bond valence (Z_B), and electron density (n) for pure elements, and V_m, n, and $\sqrt{B/V_m}$ for Al-3.125X at. % solutions.*

Alloying element (X)	Pure elements			Al-3.125 at. % X		
	V (Å^3/atom)	Z_B (el/atom)	n (el/a.u.^{3})	V_m (10^{-6} m^3/mol)	$n_{Al_{31}X}$ (el/a.u.^{3})	$\sqrt{B/V_m}$
Al	16.477	2.76	1.13	8.761	1.129	2.974
Co	10.877	3.09	1.917	8.552	1.16	4.955
Cu	12.029	2.57	1.442	8.662	1.139	3.976
Fe	11.377	3.32	1.969	8.548	1.164	4.677
Ge	24.174	-	-	8.805	-	-
Hf	22.277	3.97	1.203	8.862	1.131	3.574
Mg	22.851	2.08	0.614	8.843	1.11	2.029
Mn	10.988	3.41	2.094	8.565	1.163	4.936
Ni	10.941	2.83	1.746	8.587	1.152	4.75
Si	20.445	-	-	8.719	-	-
Sr	54.533	2.32	0.287	9.207	1.069	1.116
Ti	17.119	3.2	1.261	8.744	1.136	3.656
V	13.209	3.45	1.763	8.672	1.149	4.645
Y	32.925	3.21	0.658	9.04	1.099	2.127
Zn	15.318	2.4	1.057	8.743	1.126	2.501
Zr	23.428	3.75	1.08	8.89	1.124	3.298

The calculated results are listed in Table 4 including the bond valence, $Z_B = nV$ [42-44] where V is the volume per atom of the ground state elemental metal at 0 K. A linear relationship between $\sqrt{B/V_m}$ and $n_{Al_{31}X}$ is shown in Figure 8, i.e. $n_{Al_{31}X} = 1.0594 + 0.0207\sqrt{B/V_m}$, which allows us to predict bulk modulus from electron density and volume.
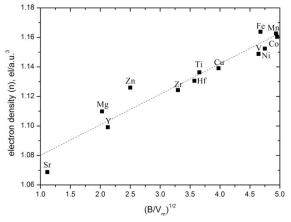

Figure 8. *Linear relationship between n and (B/Vm)1/2 of Al-3.125 at. % X solution.*

4. Summary

The effects of alloying elements (Co, Cu, Fe, Ge, Hf, Mg, Mn, Ni, Si, Sr, Ti, V, Y, Zn and Zr) on elastic properties of Al have been investigated by an efficient first-principles stress-strain method. A good agreement is obtained between calculated and available experimental data. The elastic properties of polycrystalline aggregates including bulk modulus (B), shear modulus (G), Young's modulus (E), and B/G ratio are determined based on the calculated elastic stiffness. It is found that (i) the bulk moduli of Al alloys decrease with increasing volume caused by alloying elements and (ii) the bulk modulus is also related to the total molar volume (V_m) and electron density with the relationship of $n_{Al_{31}X} = 1.0594 + 0.0207\sqrt{B/V_m}$.

References

[1] J.R. Davis, R. Joseph, In: ASM Specialty Handbook: ASM International; 1993.

[2] G.E. Totten, M. D.S., In, New York: Marcel Dekker; 2003.

[3] Z.K. Liu, Journal of Phase Equilibria and Diffusion, 30 (2009) 517-534.

[4] Y. Du, S.H. Liu, L.J. Zhang, H.H. Xu, D.D. Zhao, A.J. Wang, L.C. Zhou, CALPHAD, 35 (2011) 427-445.

[5] J. Wang, S.L. Shang, Y. Wang, Z.G. Mei, Y.F. Liang, Y. Du, Z.K. Liu, CALPHAD, 35 (2011) 562-573.

[6] D.G. Clerc, H.M. Ledbetter, J. Phys. Chem. Solids, 59 (1998) 1071.

[7] Z.K. Liu, H. Zhang, S. Ganeshan, Y. Wang, S.N. Mathaudhu, Scripta Materialia, 63 (2010) 686-691.

[8] D. Music, J.M. Schneider, Phys. Rev. B, 74 (2006).

[9] C.L. Zhang, P.D. Han, J.M. Li, M. Chi, L.Y. Yan, Y.P. Liu, X.G. Liu, B.S. Xu, J. Phys. D. Appl. Phys., 41 (2008) 095410.

[10] D.E. Kim, S.L. Shang, Z.K. Liu, Intermetallics, 18 (2010) 1163-1171.

[11] S. Ganeshan, S.L. Shang, Y. Wang, Z.K. Liu, Acta Mater., 57 (2009) 3876-3884.

[12] D. Kim, S.L. Shang, Z.K. Liu, Comp. Mater. Sci., 47 (2009) 254-260.

[13] S.L. Shang, Y. Wang, Z.K. Liu, Appl. Phys. Lett., 90 (2007) 101909.

[14] G. Kresse, J. Furthmuller, Phys. Rev. B, 54 (1996) 11169-11186.

[15] G. Kresse, J. Furthmuller, Comp. Mater. Sci., 6 (1996) 15-50.

[16] P.E. Blöchl, Phys. Rev. B, 50 (1994) 17953-17979.

[17] G. Kresse, D. Joubert, Phys. Rev. B, 59 (1999) 1758-1775.

[18] J.P. Perdew, K. Burke, M. Ernzerhof, Phys. Rev. Lett., 77 (1996) 3865-3868.

[19] M. Methfessel, A.T. Paxton, Phys. Rev. B, 40 (1989) 3616-3621.

[20] P.E. Blöchl, O. Jepsen, O.K. Andersen, Phys. Rev. B, 49 (1994) 16223-16233.

[21] H.J. Monkhorst, J.D. Pack, Phys. Rev. B, 13 (1976) 5188-5192.

[22] S.L. Shang, Y. Wang, D. Kim, Z.K. Liu, Comp. Mater. Sci., 47 (2010) 1040-1048.

[23] Y. Le Page, P. Saxe, Phys. Rev. B, 65 (2002) 104104.

[24] G. Simmons, H. Wang, In: M.I.T Press, Cambridge; 1971.

[25] H. Zhang, S.L. Shang, Y. Wang, A. Saengdeejing, L.Q. Chen, Z.K. Liu, Acta Mater., 58 (2010) 4012-4018.

[26] S.L. Shang, A. Saengdeejing, Z.G. Mei, D.E. Kim, H. Zhang, S. Ganeshan, Y. Wang, Z.K. Liu, Comp. Mater. Sci., 48 (2010) 813-826.

[27] S. Ganeshan, S.L. Shang, H. Zhang, Y. Wang, M. Mantina, Z.K. Liu, Intermetallics., 17 (2009) 313-318.

[28] A. Tonejc, A. Bonefaci, J. Appl. Phys., 40 (1969) 419-420.

[29] A. Bendijk, R. Delhez, L. Katgerman, T.H. Dekeijser, E.J. Mittemeijer, N.M. Vanderpers, J. Mater. Sci., 15 (1980) 2803-2810.

[30] A. Tonejc, A. Bonefaci, Scripta Metallurgica, 3 (1969) 145-148.

[31] Y. Wang, S. Curtarolo, C. Jiang, R. Arroyave, T. Wang, G. Ceder, L.Q. Chen, Z.K. Liu, CALPHAD, 28 (2004) 79-90.

[32] T. Wang, L.Q. Chen, Z.K. Liu, Metall. Mater. Trans. AMetall. Mater. Trans. A-Phys. Metall. Mater. Sci., 38A (2007) 562-569.

[33] U. Scheuer, B. Lengeler, Phys. Rev. B, 44 (1991) 9883-9894.

[34] R.F.S. Hearmon, Rev. Mod. Phys., 18 (1946) 409-440.

[35] C. Gault, A. Dauger, P. Boch, Physica Status Solidi a-Applied Research, 43 (1977) 625-632.

[36] H. Ledbetter, Physica Status Solidi B-Basic Research, 181 (1994) 81-85.

[37] M. Born, K. Huang, Dynamical Theory of Crystal Lattices, Oxford University Press; 1988.

[38] J.F. Nye, Physical Properties of Crystals: Their Representation by Tensors and Matrices, New York: Oxford University Press; 1985.

[39] S.F. Pugh, Phil. Mag., 45 (1954) 823-843.

[40] A.R. Miedema, F.R. Deboer, P.F. Dechatel, J. Phys. F. Met. Phys., 3 (1973) 1558-1576.

[41] C.H. Li, P. Wu, Chem. Mater., 13 (2001) 4642-4648.

[42] J.H. Rose, H.B. Shore, Phys. Rev. B, 43 (1991) 11605-11611.

[43] J.H. Rose, H.B. Shore, Phys. Rev. B, 48 (1993) 18254-18256.

[44] J.H. Rose, H.B. Shore, Phys. Rev. B, 49 (1994) 11588-11601.

[45] P. Villars, L.D. Calvert, In, ASM International, Materials Park, Ohio; 1991.